

ARTICLE

Application of quantitative protein mass spectrometric data in the early predictive analysis of target engagement by monoclonal antibodies

Morris Muliaditan¹ | Armin Sepp² 

¹Leiden Experts on Advanced Pharmacokinetics and Pharmacodynamics (LAP&P), Leiden, The Netherlands

²Simcyp Division, Certara UK Ltd., Sheffield, UK

Correspondence

Armin Sepp, Simcyp Division, Certara UK Ltd., 1 Concourse Way, Level 2-Acero, Sheffield, S1 2BJ, UK.
Email: armin.sepp@certara.com

Funding information

No funding was received for this work.

Abstract

Model-informed drug discovery is endorsed by the US Food and Drug Administration (FDA) to improve the flow of medicines from bench to bedside. In the case of monoclonal antibodies, this necessitates taking into account not only the pharmacokinetic (PK) properties of the drug, but also the tissue distribution, concentration, and turnover of the target to guide dose and affinity selection, as well as serve as a link to downstream pharmacology. Relevant information (e.g., tissue proteomic data from quantitative mass spectrometry), is increasingly available from public domain data repositories, although not necessarily in the form that is directly usable for the purpose of quantitative, predictive, and mechanistic PK/pharmacodynamic (PD) modeling based on molarity or similar frameworks instead. Using secreted plasma protein concentrations measured both by immunochemical methods and mass spectrometry, we addressed this gap and derived an optimized nonlinear empirical function that establishes the correlation between the two data sets and validated the approach taken using a wider data set of all proteins found in plasma. In addition, we present a semimechanistic framework for the plasma half-life of soluble proteins where clearance is expressed as a nonlinear function of the molecular weight of the protein. Finally, we apply the approach to two established therapeutic antibody targets: complement factor C5 and PCSK9 to demonstrate how the described framework can be applied to predictive PK/PD modeling.

Study Highlights**WHAT IS THE CURRENT KNOWLEDGE ON THE TOPIC?**

Model-informed drug development paradigm is increasingly being applied from the earliest stages of the development of novel monoclonal antibodies in order to improve the success rate in the clinic but this can be limited by the availability of relevant biochemical information.

This is an open access article under the terms of the [Creative Commons Attribution-NonCommercial-NoDerivs](https://creativecommons.org/licenses/by-nc-nd/4.0/) License, which permits use and distribution in any medium, provided the original work is properly cited, the use is non-commercial and no modifications or adaptations are made.

© 2022 The Authors. *Clinical and Translational Science* published by Wiley Periodicals LLC on behalf of American Society for Clinical Pharmacology and Therapeutics.

WHAT QUESTION DID THIS STUDY ADDRESS?

We looked at the alternative ways for estimating target concentrations and turnover when there are little to no biochemical data available and related that to the dose and affinity of the mAb.

WHAT DOES THIS STUDY ADD TO OUR KNOWLEDGE?

We demonstrate that it is feasible to derive target concentrations and estimate plasma protein turnover from quantitative protein mass spectrometric data and molecular weight-based semimechanistic renal clearance modeling, respectively.

HOW MIGHT THIS CHANGE CLINICAL PHARMACOLOGY OR TRANSLATIONAL SCIENCE?

This approach allows the evaluation of target druggability as well as setting the criteria for the desired monoclonal antibody affinity and efficacious human dose at the earliest stage of drug discovery.

INTRODUCTION

Monoclonal antibodies (mAbs) are widely used in the clinic for the treatment of diseases ranging from immuno-inflammation to oncology.^{1,2} Despite the need and necessity, the discovery and development of novel drugs, including mAbs, remains time-consuming, expensive,³ and prone to attrition.⁴ Model-informed drug development (MIDD) paradigm has been endorsed by the US Food and Drug Administration (FDA) to encourage the application of quantitative modeling and simulation from the earliest stages of drug discovery in order to improve the success rate of new medicines later in the clinic.⁵ This is especially relevant in the case of mAbs, where target-related interactions can drastically affect the elimination of the drug with consequences for downstream pharmacology. Quantitative analysis of these processes requires taking into account the concentrations and turnover of the target, as well as the affinity and dosing of the drug itself. Although often available from biochemical studies, recent advances in quantitative mass spectrometry have extended significantly the data available to cover most of the proteome, including parts of it that are less amenable to earlier methods. Whereas potentially highly valuable, the mass spectrometric data do not necessarily come in the form that can be directly incorporated into pharmacokinetic/pharmacodynamic (PK/PD) modeling where molar concentrations are of critical importance as the pillars of mass action kinetics.

We demonstrate that this difficulty can be overcome by establishing an empirical quantitative correlation between the “parts per million” (ppm) mass spectrometric plasma protein abundance information from the PaxDb database⁶ and biochemically measured respective molar concentration values. For target turnover of plasma proteins, we suggest incorporating information from stable

isotope labelling with amino acids in cell culture studies of protein turnover and hydrodynamic radius-dependent renal clearance.

We used complement C5 and proprotein convertase subtilisin/kexin type 9 (PCSK9) as paradigm targets to illustrate how this framework, within a single-compartment drug-ligand binding model,⁷ can be used to support realistic decision making for mAbs at the early stages of drug discovery. We suggest that this approach can be useful whenever target abundance and turnover are likely to have a significant effect on the PK/PD profile of the drug as well as the target.

METHODS

Source of protein levels in human plasma

Human plasma protein concentrations were downloaded from public databases⁸⁻¹¹ and converted to nM using predicted molecular weight from UniProt,¹² except for Wiśniewski et al.,¹¹ which were already in nM. In addition, we classified each protein according to their predicted location (intracellular, membrane, and/or secreted) as reported by the Human Protein Atlas database (version 21.0).¹³ Plasma protein mass spectrometric abundance values were downloaded from the PaxDb database created by Wang et al.⁶

Inclusion/exclusion criteria for the prediction of protein levels in human plasma

Only secreted plasma protein “integrated” data were used to establish the correlation between ppm and molarity, as these represent the consensus estimates. Plasma proteins

with missing or duplicated concentrations were removed, as well as proteins for which the molecular weight was not available from UniProt. Validation of the predictive performance of the model was subsequently performed using the other proteins from the above data set, except for intracellular proteins.

Software

Modeling and statistical analysis was performed using a nonlinear mixed effect approach as implemented in NONMEM version 7.5.¹⁴ Pre and postprocessing of data, as well as simulations were performed in R version 4.1.1.¹⁵ Literature data were digitized using WebPlotDigitizer.¹⁶

Prediction of protein levels in human plasma

Mass spectrometric ppm concentration values vary by about 7.5 orders of magnitude in the data set used, while for the biochemical molar concentration values the range is almost nine. Both a linear regression (Equation 1) and sigmoidal-shape model (Equation 2) were tested to describe the relationship between ppm and molar concentrations:

$$\log_{10}(\text{nM}) = \text{Int} + \text{slope} \cdot \log_{10}(\text{ppm}) \quad (1)$$

$$\log_{10}(\text{nM}) = \frac{(\text{Base} + \text{MaxDV}) \cdot \text{ppm}^{\text{hill}}}{\text{ppm}50^{\text{hill}} + \text{ppm}^{\text{hill}}} - \text{Base} \quad (2)$$

whereby Int represents the intercept of the linear regression model, Base and MaxDV the minimum and maximum predicted protein concentrations (in nM), respectively, and ppm50 the ppm value whereby predicted concentrations are 50% of MaxDV. Additive residual error (on the log₁₀ transformed protein concentrations) was used (Equation 3):

$$y = \text{PRED} + \varepsilon(1) \quad (3)$$

whereby PRED represents the population predicted concentration (in log₁₀ nM) and ε the estimated residual error which is assumed to follow a normal distribution with mean zero and variance σ^2 .

The goodness of fit was evaluated visually, by parameter precision (relative standard error) and Akaike Information Criterion (AIC),¹⁷ which was calculated using Equation 4:

$$\text{AIC} = \text{OFV} + 2 \cdot P \quad (4)$$

where OFV represents the minimum objective function value and P the number of model parameters.¹⁸ The model with the lowest AIC was considered the superior model. The relative likelihood (RL) of the models was subsequently derived from AIC using Equation 5.

$$\text{RL}_i = \exp(0.5 \cdot (\text{AIC}_{\text{min}} - \text{AIC}_i)) \quad (5)$$

Prediction of protein half-life in human plasma

Plasma protein half-life was analyzed in terms of protein size-dependent elimination by renal filtration and size-independent default elimination, as previously described by Sepp et al.¹⁹ Renal elimination was described as a function of protein size, where a_e is its hydrodynamic radius in nm, MW denotes molecular weight in kDa, and Θ represents the glomerular filtration coefficient¹⁹:

$$a_e = 0.5614 \sqrt[3]{\text{MW}} + 0.09611 \sqrt[2]{\text{MW}} \quad (6)$$

$$\Theta = \frac{1}{\left(1 + \left(\frac{a_e}{2.95}\right)^{7.11}\right)^{3.8}} \quad (7)$$

$$k_{\text{elim}} = \frac{\Theta \cdot \text{GFR}}{V_{\text{ss}}} + k_{\text{elim},0} \quad (8)$$

$$t_{1/2} = \frac{\ln(2)}{k_{\text{elim}}} \quad (9)$$

The protein default elimination rate constant (k_{elim}) was calculated from the predicted glomerular filtration coefficient using human glomerular filtration rate (GFR) value of 8400 ml/h²⁰ and postulating the volume of distribution (V_{ss}) as 6000 ml that is typical for therapeutic antibodies.²¹ An intrinsic elimination rate constant ($k_{\text{elim},0}$) of 0.00693 1/h was added for the equation to yield the half-life of around 100 h for proteins with the glomerular filtration coefficient close to zero (e.g., what IgG would have in FcRn-saturating conditions), when macropinocytosis, a nonspecific clearance pathway, dominates.²²⁻²⁴

The macropinocytosis-predicted half-life should be considered as an upper threshold value (i.e., the observed protein half-lives may be faster than predicted by the model), if proteolytic degradation or receptor-mediated clearance are significant. The correlation between protein half-life and molecular weight by Kontermann²⁵ and Strohl²⁶ were used to assess the model performance to predict human plasma protein half-life from the molecular weight. It should be noted that it is the molecular weight of the circulating protein, and if information is available

for any relevant post-translational modifications like glycosylation or dimerization, that should be factored in.

Example: Application of the modeling framework for early human dose prediction for a human complement C5- and PCSK9 neutralizing mAbs

A quasi-steady-state drug-ligand binding kinetic model⁷ was used for the PK/PD simulations (Figure S1). The model consists of a system of differential equations to describe the change of drug, free target, and complex concentrations over time in a two-compartment framework. Disposition parameters in humans were assumed to follow published typical values²¹ (Table S1). The complex elimination rate (k_{int}) was assumed to be the same as the mAb elimination rate (k_{el}).²⁷ Baseline levels and turnover of C5 and PCSK9 in human plasma was predicted by the aforementioned models and compared with literature values.

The C5 inhibition was analyzed at a range of dosing regimens and intervals typical for therapeutic mAbs (every 7, 14, and 28 days as 1 h intravenous [i.v.] infusions). PCSK9 inhibition was analyzed at similar dosing regimens and intervals, but administered as subcutaneous (s.c.) injections. Absorption parameters were assumed to follow published typical values (Table S1).²⁸ Sensitivity analysis was performed using the median predicted system parameters as well as assuming a worst-case scenario of higher than predicted baseline levels or faster turnover on the predicted target inhibition. The optimal human dose was selected based on the dosing regimen that was deemed to have the best likelihood of achieving a target inhibition of $\geq 95\%$ in the clinic.

RESULTS

Correlation between mass spectrometric and biochemical estimates for plasma protein in humans

In total, there was mass spectrometric data for 4086 plasma proteins in the PaxDb database with UniProt ID available, whereas biochemical assays provided data for 3651 proteins with 4900 concentration values. After application of the exclusion criteria, the combined final human plasma proteome dataset contained 2457 mass spectrometric ppm values (i.e., 2457 unique proteins) and 3643 biochemical measurements (Figure S2). Of these, 555 plasma concentrations from 274 proteins that were classified as secreted proteins were used for model training, whereas the

remaining proteins (except intracellular) were reserved for model validation purposes.

Parameter estimates for both the linear and sigmoidal models are shown in Table 1. As shown in Figure 1, both the linear and sigmoidal models performed well for proteins in the medium concentration range. However, the latter captured better the data at extremes (Figure 1). This was reflected in the lower AIC value for the sigmoidal versus linear model (230.39 vs. 293.36, respectively) and in the better goodness of fit plot (Figure S3). The relative likelihood of the linear model being better than the sigmoidal one was calculated as $2.12E-14$ (i.e., the sigmoidal model provides significantly better overall correlation for the two data sets), principally due to the large data set and wide dynamic range of the values available. External validation of the model using the other proteins found in plasma (e.g., the shed extracellular domains of membrane proteins and intracellular proteins released on cell lysis), demonstrated good predictive performance of the sigmoidal model (Figure 2). Likewise, the plasma concentration predictions were also within two-fold (11 out of 17) or four-fold (16 out of 17) of reported literature values for some of the current therapeutic mAb targets, suggesting good performance of the sigmoidal-shaped empirical correlation for clinically relevant targets (Figure 3).

Turnover of plasma proteins in humans

The empirical Equation 8 postulates two independent pathways of elimination for plasma proteins. First,

TABLE 1 Overview of model parameter estimates describing the correlation between ppm and plasma concentrations for soluble proteins using a linear and sigmoidal model

Parameter	Estimate [%RSE]
Linear model	
Objective function, OFV	289.36
Intercept, log ₁₀ nM	0.948 [6.89]
Slope	1.035 [2.66]
Additive residual error on log ₁₀ scale, σ^2	0.620 [8.16]
Sigmoidal model	
Objective function, OFV	222.39
Base, log ₁₀ nM	2.533 [14.0]
Hill	0.275 [15.8]
ppm ₅₀	267.55 [64.4]
MaxDV, log ₁₀ nM	5.60 [15.0]
Additive residual error on log ₁₀ scale, σ^2	0.549 [7.75]

Abbreviations: MaxDV, maximum predicted protein concentrations; OFV, objective function value; ppm, parts per million; RSE, relative standard error.

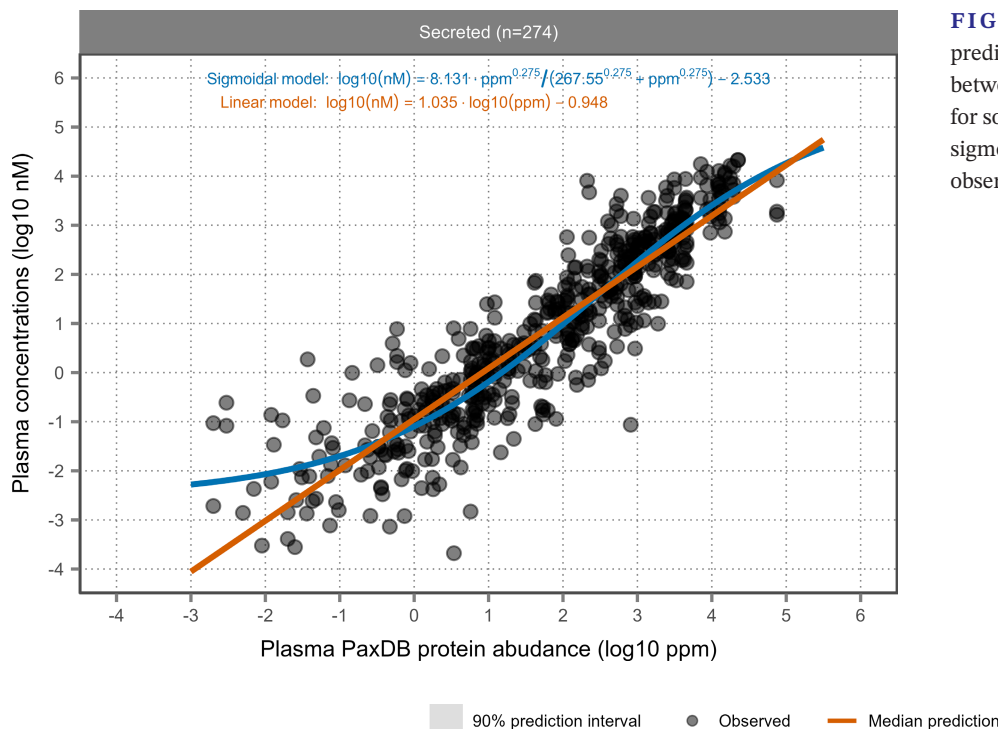


FIGURE 1 Comparison of the predicted correlation (solid lines) between ppm and plasma concentrations for soluble proteins using a linear and sigmoidal model. Circles represent the observed data. ppm, parts per million

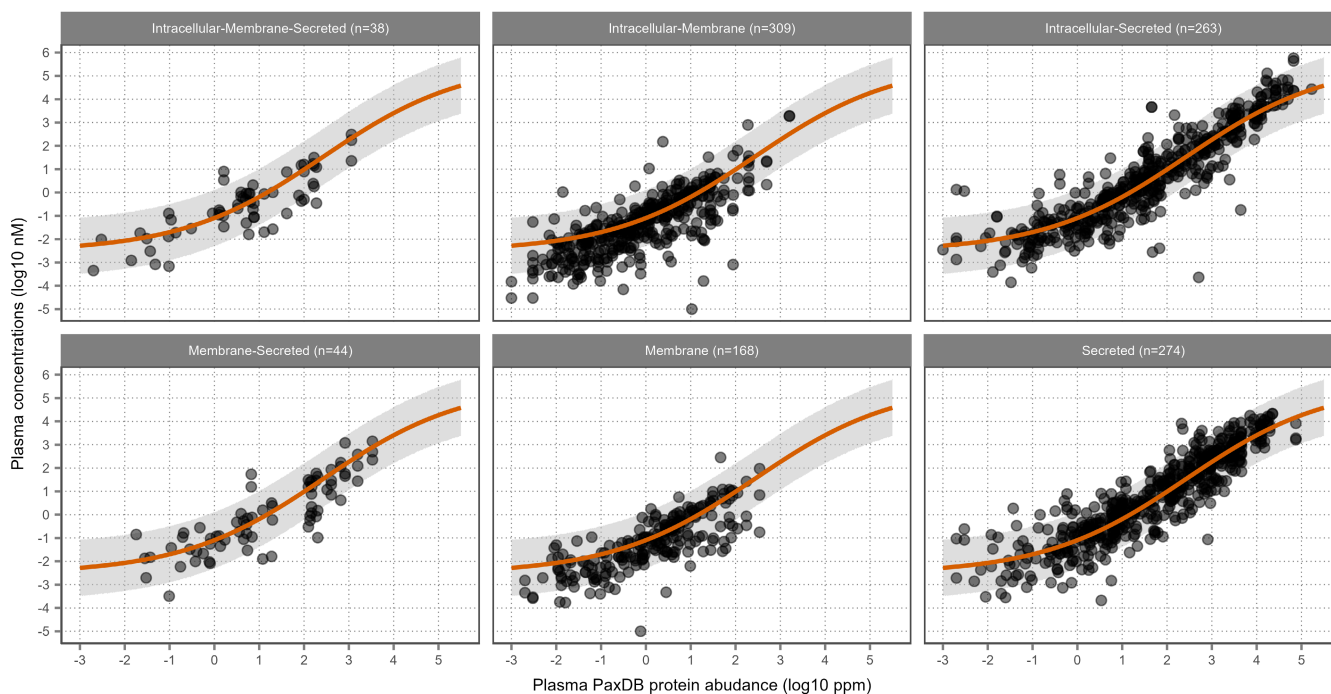


FIGURE 2 External validation of the sigmoidal model to describe the relationship between ppm and plasma concentrations. One thousand simulations were performed to derive the predicted median plasma concentrations and corresponding 90% prediction interval. Secreted proteins were used as the training dataset. ppm, parts per million

there is invariant elimination with the rate constant $k_{\text{elim},0}$ that applies to all proteins and reflects the default pinocytosis-related clearance. Second, there is a protein size-dependent component that reflects renal elimination and depends on the hydrodynamic size of the protein. This pathway contributes increasingly as

the molecular weight of the protein decreases below ~60 kDa renal filtration cutoff value. This approach proved to be an adequate prediction of plasma protein turnover (Figure 4) except for albumin and IgG, which are subject to FcRn mediated half-life extending endosomal recycling.

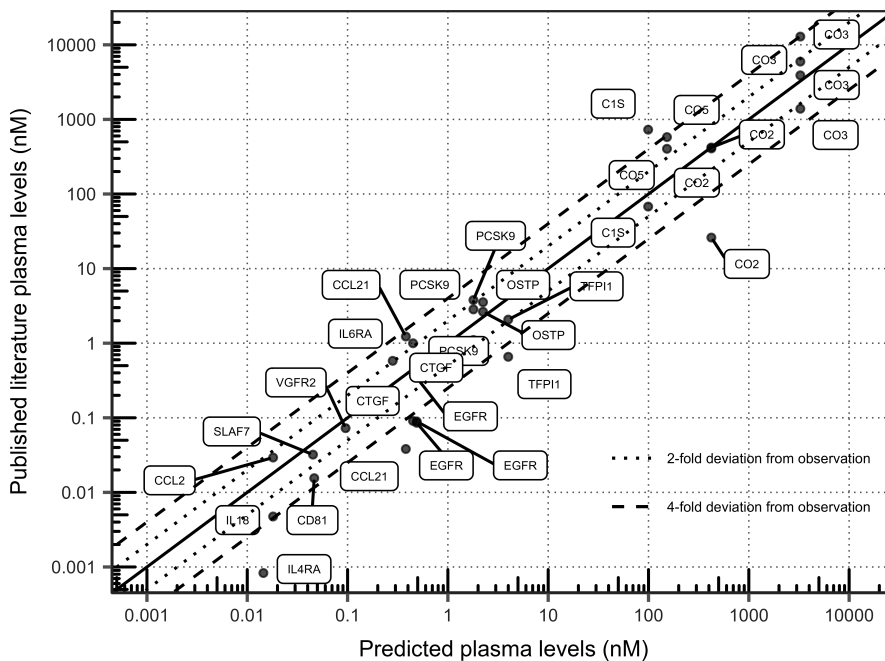


FIGURE 3 Predicted versus observed plasma concentrations of some of the current therapeutic mAb targets. Dotted lines represent a two-fold or four-fold deviation from the observed value. C1S, complement C1s subcomponent; CCL2, C-C motif chemokine 2; CCL21, C-C motif chemokine 21; CD81, CD81 antigen; CO2, complement C2; CO3, complement C3; CO5, complement C5; CTGF, CCN family member 2; EGFR, epidermal growth factor receptor; IL18, interleukin-18; IL4RA, interleukin-4 receptor subunit alpha; IL6RA, interleukin-6 receptor subunit alpha; OSTP, osteopontin; PCSK9, proprotein convertase subtilisin/kexin type 9; SLAF7, SLAM family member 7; TFP11, tissue factor pathway inhibitor; VGFR2, vascular endothelial growth factor receptor 2

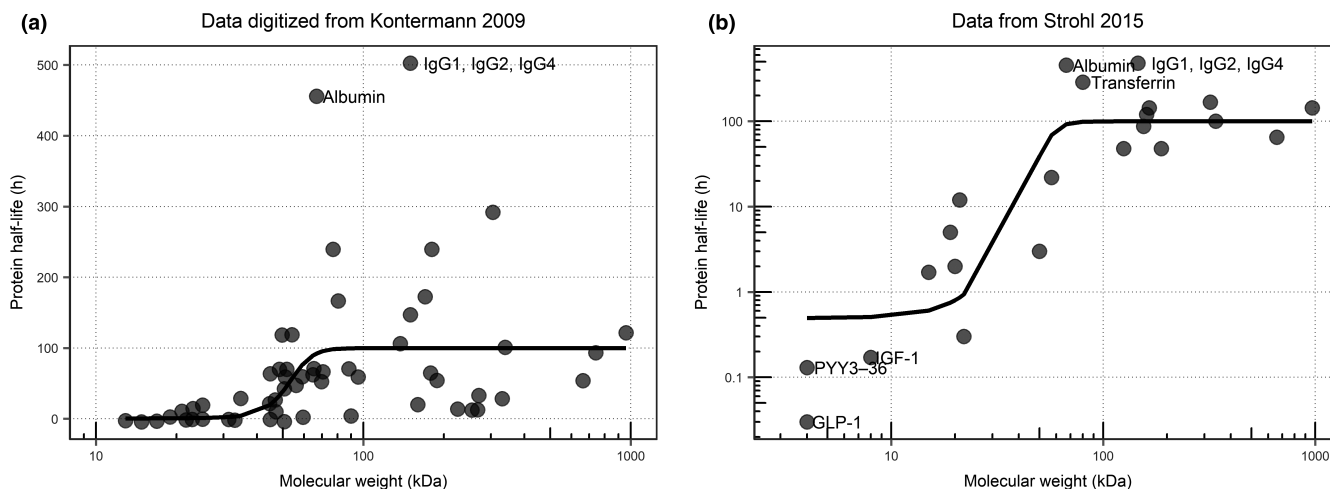


FIGURE 4 Predicted (solid line) versus observed (circles) correlation between protein half-life and molecular weight in human plasma. Observed protein half-lives were digitized from Kontermann²⁵ (a) or Strohl²⁶ (b). GLP, glucagon-like peptide; IGF, insulin-like growth factor; PYY, peptide tyrosine tyrosine

Example 1: Application of the modeling framework to early assessment of human dose for a complement C5-neutralizing mAb

The sigmoidal concentration correlation model predicted a C5 plasma baseline level of 153 (90% prediction interval

[PI]: 9.9–2438) nM, whereas the half-life was assigned as 100h (due to a high molecular weight of 190kDa). At these values, the drug-ligand binding model prediction for the human dose for an anti-C5 mAb with KD of 100 pM that would be required to achieve >95% reduction in free C5 relative to the pre-dosing levels was ≥ 3 mg/kg q7d or ≥ 6 mg/kg q14d or ≥ 20 mg/kg q28d (Figure 5a). By way of

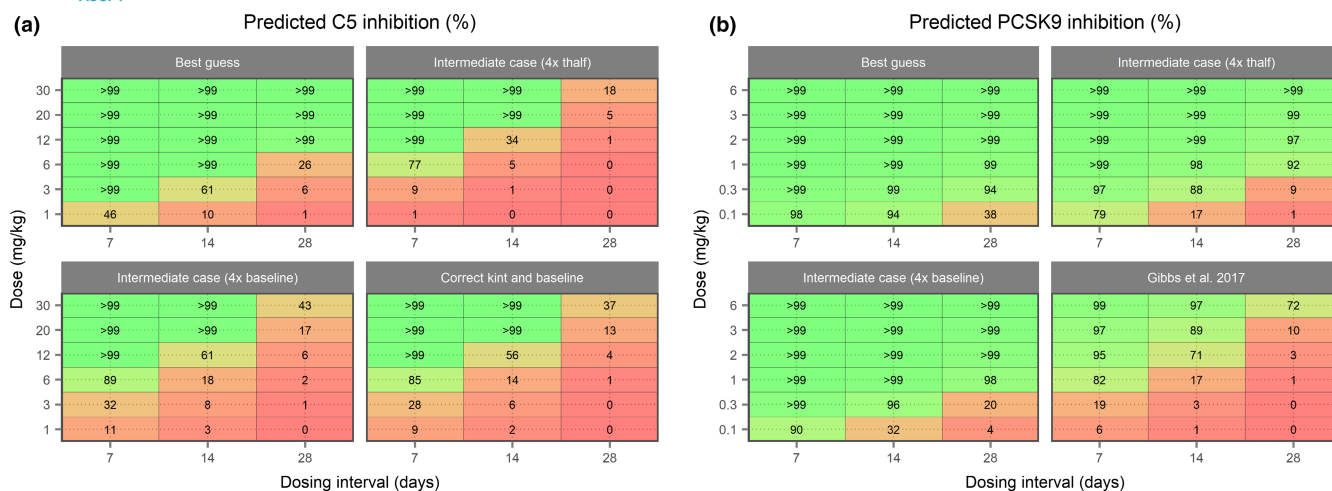


FIGURE 5 Predicted dosing interval versus dose and C5 (a) or PCSK9 (b) inhibition at trough using the proposed modeling framework. Target engagement (numbers shown in each cell) was predicted under different scenarios

sensitivity analysis, if one allows for the four-fold higher plasma concentration (which appears to be a reasonable assumption based on Figure 3) than that predicted from the model or four-fold shorter half-life, the required dose will increase proportionally to ≥ 12 mg/kg q7d or ≥ 20 mg/kg q14d (Figure 5a).

The recommended efficacious human dose was, subsequently, compared with the therapeutic dose of the approved anti-C5 mAb (eculizumab) from a phase III clinical trial in patients with paroxysmal nocturnal hemoglobinuria (PNH).²⁹ The clinically efficacious maintenance dose of 12–15 mg/kg q14d lies between the two model-based scenarios described above. Some discrepancy was observed between the predicted and observed total C5 following eculizumab administration (Figure S4). Sensitivity analyses revealed that the uncertainty was mainly due to the bias of the baseline C5 level prediction (although the true value falls within the range of simulation scenarios) and the k_{deg}/k_{int} ratio, as the half-life of eculizumab is reduced when bound to C5. This insight would not be known at the early assessment stage. The predicted half-life of C5 was close to the reported clinical value (100 h vs. 85 h, respectively, due to the large size of the protein at 190 kDa molecular weight). If the biochemical assay value had been adopted for the plasma concentration of C5, the model would have been able to predict the PK/PD correlation almost correctly (Figure S4). There is no statistically significant difference between plasma C5 concentrations in healthy patients and in patients with PNH (103 ± 19 vs. 133 ± 38 mg/ml, respectively)³⁰ and in therapeutic application the plasma concentration of free C5 is reduced to $<5\%$ of the predosing level for efficacy.³⁰

Example 2: Application of the modeling framework to early assessment of human dose for a human PCSK9-neutralizing mAb

The sigmoidal concentration correlation model predicted a PCSK9 plasma baseline level of 1.88 (90% PI: 0.11–29.7) nM, whereas the half-life was assigned as 97.5 h based on its molecular weight (74 kDa). At these values, the drug-ligand binding model prediction for the human dose for an anti-PCSK9 mAb with KD of 100 pM that would be required to achieve $>95\%$ reduction in free PCSK9 relative to the predosing levels was ≥ 0.1 mg/kg q7d or ≥ 0.3 mg/kg q14d or ≥ 1 mg/kg q28d (Figure 5b). By way of sensitivity analysis, if one allows for the four-fold higher plasma concentration than that predicted from the model or four-fold shorter half-life, the required dose was predicted to increase to ≥ 0.3 mg/kg q7d or ≥ 1 mg/kg q14d or ≥ 2 mg/kg q28d (Figure 5b).

The recommended efficacious human dose was, subsequently, compared with the therapeutic dose of an approved anti-PCSK9 mAb (evolocumab), which is either 140 mg or 420 mg q28d³¹ (i.e., equivalent to 2 mg/kg q14d or 6 mg/kg q28d for a typical 70 kg subject). The predicted PCSK9 plasma baseline level (1.88 nM) was comparable to published estimated value in healthy subjects (3.36 nM).³² Baseline levels in patients with hypercholesterolemia stably treated with statins (5.27 nM)³² was underpredicted, but still fell within the four-fold uncertainty range, that was included in the sensitivity analysis. On the other hand, the reported half-life of PCSK9 in human (7.8 h)³² was faster than the predicted half-life (97.5 h), due to low-density lipoprotein receptor (LDLR) mediated clearance. Complex elimination rate (k_{int}) was reported to be 0.0022 1/h,³² which was quite close to the model initial

assumption ($k_{\text{int}} = k_{\text{el}} = 0.0032$ 1/h). Nevertheless, despite the discrepancies between the initial assumed and published estimated PCSK9 plasma baseline level and half-life, it can be concluded that the proposed MIDD approach still led to predicted human doses that were quite close to the current therapeutic doses.

DISCUSSION

Prediction of plasma protein concentration and turnover

Target protein abundance and turnover are two key parameters required for the analysis of target druggability and, in this work, we are proposing an early target druggability assessment scheme based on both. Most notably, we find there to be good correlation between the concentration values from biochemical assays and mass spectrometric measurements that span seven orders of magnitude range. Often a range of values from different laboratories is available,^{8–11} so that the most likely one can be identified. The approach described by us is most useful if only mass spectrometric values are available and potentially in cases where dynamic changes in plasma proteome composition in response to the drug is analyzed for PD purposes and converted into biochemically more usable molarity concentrations.

When the target concentration estimate is combined with turnover and clearance, the empirical framework presented can be used to analyze the likely dosing range for an antibody of given affinity. If there are unaccounted specific or nonspecific clearance pathways in operation in addition to glomerular filtration and macropinocytosis, the net result would be shorter than the model-predicted half-life and higher than expected accumulation of the complex with the mAb. In this case, dose elevation and/or affinity maturation of the mAb may need to be considered for maintaining the desired threshold level of free target. Likewise, if the protein target dimerizes in solution, it is the molecular weight of the dimer that is used for glomerular filtration, as well as any other post-translational modification that affects molecular weight (e.g., glycosylation).

The observed nonlinearity between mass spectrometric ppm and biochemical molarity values is more strongly pronounced in the case of low concentration proteins present in the plasma in the picomolar range (e.g., cytokines), where the assays are pushed to their sensitivity limits. Even with this caveat, the model accurately predicted the validation data sets where the extended plasma proteome was analyzed. A <4-fold deviation for a set of therapeutically relevant targets confirms good overall performance of the model.

Second, we propose an empirical function which relates the plasma half-life of proteins to its molecular weight. Equation 8 is parameterized to yield a half-life of around 100h for proteins with a molecular weight >67kDa, which are not subject to renal elimination or FcRn-mediated recycling, whereas the smaller proteins are progressively rapidly removed through the kidneys as their size decreases. As a result, the presented model can be used to predict plasma protein turnover in cases where such information is not available from public of databases.^{33,34} It is important to notice that this does not take into account more specific clearance pathways which may decrease the half-life further still, for example, proteolytic degradation or internalization through membrane-bound interaction partners, such as PCSK9, for which the reported human half-life was shorter than predicted. In this case, the discrepancy could be explained by the fact that current approach does not account for PCSK9 internalization through binding with LDLR. This would manifest itself through more extensive accumulation of the mAb complex than expected from the predicted half-life and predosing target level alone, requiring the presence of the mAb at higher concentration or better affinity for the desired therapeutic outcome.

Application of the modeling framework

Using complement C5 and PCSK9 as an example, we showed that it is possible to closely predict the anticipated efficacious human dose by using the quantitative modeling approach described here, at the early stages of drug discovery already. Despite some discrepancy in the predicted and observed total C5, the predicted human dose based on a hypothetical 100 pM mAb (based on achieving >95% C5 inhibition observed in the clinical setting, and supported by similar reduction of C5 convertase turnover in self-amplified *in vitro* reactions),^{35–37} closely correlated with current therapeutic doses of eculizumab (840 mg q7d for 70 kg subject vs. 600–900 mg q7d). Similar results were achieved with PCSK9, where predicted human doses were quite close to current therapeutic doses of evolocumab. These findings suggest that despite the simplicity and assumptions made, including constant expression rate of the target, the approach described can be informative in the MIDD process from the earliest stages even before any lead molecule is generated and tested, due to the practical limitations of doses that can be given in the clinic. Likewise, if the desired free target threshold level is known, an assessment can be made for the affinity requirement of the mAb for a given dose.

LIMITATIONS

The correlation between mass spectrometric and biochemical protein concentration estimates across the entire data set that covered around eight orders of magnitude, is significant but is also associated with statistical uncertainty. Due to the large variability in the data, 90% PI across the ppm range covered approximately two orders of magnitude on log₁₀ scale (i.e., 100-fold), which is a major caveat that needs to be considered during modeling. Likewise, tissue distribution and accessibility to mAbs may not be reflected sufficiently in a very simple model used herein whereas the overall dose will also depend on the threshold level of free target level that must be achieved and maintained, as well as the affinity of the mAb. The desired free target levels may be below predosing normal and/or healthy levels as in the C5 and PCSK9 example given but this is ultimately determined by the etiology of the disease and independent mechanistic insight available. In addition, it should be noted that baseline levels and turnover are predicted using literature data measured in healthy volunteers, which may deviate from levels in patients. It is therefore important for modelers to always keep the target biology, including differences between healthy and disease conditions, in mind when performing the human dose predictions.

It is important to stress that these are early human dose predictions which one would typically perform at early lead optimization in which experimental data may not be available. To address the expected uncertainties at such an early stage, it would be prudent to regularly perform human dose predictions at a range of scenarios. In this way, the impact of the degree of uncertainty regarding target- and drug-specific parameters on the predicted efficacious human dose can be constantly taken into account for each decision making stage, whereas the knowledge gaps can decrease as more experimental data becomes available as the project moves toward the clinical stage. Further evaluation of the proposed approach to predict human dose at early lead optimization for other targets is warranted.

In summary, we have demonstrated how easily accessible information can be used in the spirit of MIDD to critically evaluate significant aspects of drug discovery, such as the likely dose and affinity of the medicine prior to lead optimization, so that effort can be focused on areas where the likelihood of success is the highest.

ACKNOWLEDGEMENTS

The authors wish to acknowledge expert help from Ms. Ruth Clayton and Ms. Eleanor Savill in preparing this

manuscript. The authors would also like to thank Tamara van Steeg for her valuable comments on the manuscript.

CONFLICT OF INTEREST

The authors declared no competing interests for this work.

AUTHOR CONTRIBUTIONS

M.M. performed the research. M.M. and A.S. wrote the manuscript, designed the research, and analyzed the data.

ORCID

Armin Sepp  <https://orcid.org/0000-0002-9276-5814>

REFERENCES

- Kaplon H, Reichert JM. Antibodies to watch in 2021. *MAbs*. 2021;13:1860476.
- Urquhart L. Top companies and drugs by sales in 2020. *Nat Rev Drug Discov*. 2021;20:253.
- Wouters OJ, McKee M, Luyten J. Estimated research and development investment needed to bring a new medicine to market, 2009-2018. *JAMA*. 2020;323:844-853.
- Dowden H, Munro J. Trends in clinical success rates and therapeutic focus. *Nat Rev Drug Discov*. 2019;18:495-496.
- Marshall SF, Burghaus R, Cosson V, et al. Good practices in model-informed drug discovery and development: practice, application, and documentation. *CPT Pharmacometrics Syst Pharmacol*. 2016;5:93-122.
- Wang M, Herrmann CJ, Simonovic M, Szklarczyk D, von Mering C. Version 4.0 of PaxDb: protein abundance data, integrated across model organisms, tissues, and cell-lines. *Proteomics*. 2015;15:3163-3168.
- Gibiansky L, Gibiansky E, Kakkar T, Ma P. Approximations of the target-mediated drug disposition model and identifiability of model parameters. *J Pharmacokinetic Pharmacodyn*. 2008;35:573-591.
- Uhlen M, Karlsson MJ, Zhong W, et al. A genome-wide transcriptomic analysis of protein-coding genes in human blood cells. *Science*. 2019;366:eaax9198.
- Farrar T, Deutsch EW, Omenn GS, et al. A high-confidence human plasma proteome reference set with estimated concentrations in PeptideAtlas. *Mol Cell Proteomics*. 2011;10:M110.006353.
- Geyer PE, Kulak NA, Pichler G, Holdt LM, Teupser D, Mann M. Plasma proteome profiling to assess human health and disease. *Cell Syst*. 2016;2:185-195.
- Wiśniewski JR, Hein MY, Cox J, Mann M. A "proteomic ruler" for protein copy number and concentration estimation without spike-in standards. *Mol Cell Proteomics*. 2014;13:3497-3506.
- Bateman A. UniProt: a worldwide hub of protein knowledge. *Nucleic Acids Res*. 2019;47:D506-D515.
- Uhlen M, Fagerberg L, Hallstrom BM, et al. Tissue-based map of the human proteome. *Science*. 2015;347:1260419.
- Beal SL, Sheiner LB, Boeckmann AJ, Bauer RJ. *NONMEM 7.5 Users Guides; 1989-2020*. Icon Development Solutions.
- R Core Team (2021). *R: A language and environment for statistical computing*. R Foundation for Statistical Computing. <https://www.R-project.org/>

16. Rohatgi A. WebPlotDigitizer: Version 4.5. Accessed May 6, 2021. <https://automeris.io/WebPlotDigitizer>
17. Akaike H. A new look at the statistical model identification. *IEEE Trans Autom Control*. 1974;19:716-723.
18. Olofson E, Dahan A. Using Akaike's information theoretic criterion in mixed-effects modeling of pharmacokinetic data: a simulation study. *F1000Res*. 2013;2:71.
19. Sepp A, Meno-Tetang G, Weber A, Sanderson A, Schon O, Berges A. Computer-assembled cross-species/cross-modalities two-pore physiologically based pharmacokinetic model for biologics in mice and rats. *J Pharmacokinet Pharmacodyn*. 2019;46:339-359.
20. Kaufman DP, Basit H, Knohl SJ. Physiology, glomerular filtration rate. In: *StatPearls*. StatPearls Publishing LLC; 2021.
21. Betts A, Keunecke A, van Steeg TJ, et al. Linear pharmacokinetic parameters for monoclonal antibodies are similar within a species and across different pharmacological targets: a comparison between human, cynomolgus monkey and hFcRn Tg32 transgenic mouse using a population-modeling approach. *MAbs*. 2018;10:751-764.
22. Waldmann TA, Terru WD. Familial hypercatabolic hypoproteinemia. A disorder of endogenous catabolism of albumin and immunoglobulin. *J Clin Invest*. 1990;86:2093-2098.
23. Kim J, Hayton WL, Robinson JM, Anderson CL. Kinetics of FcRn-mediated recycling of IgG and albumin in human: pathophysiology and therapeutic implications using a simplified mechanism-based model. *Clin Immunol*. 2007;122:146-155.
24. Waldmann TA, Strober W. Metabolism of Immunoglobulins. *Prog Allergy*. 1969;13:1-110.
25. Kontermann RE. Strategies to extend plasma half-lives of recombinant antibodies. *BioDrugs*. 2009;23:93-109.
26. Strohl WR. Fusion proteins for half-life extension of biologics as a strategy to make biobetters. *BioDrugs*. 2015;29:215-239.
27. Davda JP, Hansen RJ. Properties of a general PK/PD model of antibody-ligand interactions for therapeutic antibodies that bind to soluble endogenous targets. *MAbs*. 2010;2:576-588.
28. Dirks NL, Meibohm B. Population pharmacokinetics of therapeutic monoclonal antibodies. *Clin Pharmacokinet*. 2010;49:633-659.
29. Peffault de Latour R, Brodsky RA, Ortiz S, et al. Pharmacokinetic and pharmacodynamic effects of ravulizumab and eculizumab on complement component 5 in adults with paroxysmal nocturnal haemoglobinuria: results of two phase 3 randomised, multicentre studies. *Br J Haematol*. 2020;191:476-485.
30. Röth A, Nishimura JI, Nagy Z, et al. The complement C5 inhibitor crovalimab in paroxysmal nocturnal hemoglobinuria. *Blood*. 2020;135:912-920.
31. Kasichayanula S, Grover A, Emery MG, et al. Clinical pharmacokinetics and pharmacodynamics of evolocumab, a PCSK9 inhibitor. *Clin Pharmacokinet*. 2018;57:769-779.
32. Gibbs JP, Doshi S, Kuchimanchi M, et al. Impact of target-mediated elimination on the dose and regimen of evolocumab, a human monoclonal antibody against proprotein convertase subtilisin/kexin type 9 (PCSK9). *J Clin Pharmacol*. 2017;57:616-626.
33. Wang D, Liem DA, Lau E, et al. Characterization of human plasma proteome dynamics using deuterium oxide. *Proteomics Clin Appl*. 2014;8:610-619.
34. Mathieson T, Franken H, Kosinski J, et al. Systematic analysis of protein turnover in primary cells. *Nat Commun*. 2018;9:1-10.
35. Latha CD, Kassir N, Mouksassi MS, et al. Population pharmacodynamic/pharmacokinetic modeling of eculizumab and free complement component protein C5 in pediatric and adult patients with atypical hemolytic uremic syndrome (aHUS). Presented at the American Society for Clinical Pharmacology and Therapeutics (ASCP) Annual Meeting, Atlanta, GA March 18–22 2014; Abstract # 387. Accessed February 4, 2022. https://www.certara.com/app/uploads/Resources/Posters/ASCP_Alexion-Pharsight_Poster-2.pdf
36. Hillmen P, Hall C, Marsh JC, et al. Effect of eculizumab on hemolysis and transfusion requirements in patients with paroxysmal nocturnal hemoglobinuria. *N Engl J Med*. 2004;350:552-559.
37. Rawal N, Pangburn M. Formation of high-affinity C5 convertases of the alternative pathway of complement. *J Immunol*. 2001;166:2635-2642.

SUPPORTING INFORMATION

Additional supporting information may be found in the online version of the article at the publisher's website.

How to cite this article: Muliaditan M, Sepp A. Application of quantitative protein mass spectrometric data in the early predictive analysis of target engagement by monoclonal antibodies. *Clin Transl Sci*. 2022;15:1634-1643. doi:[10.1111/cts.13278](https://doi.org/10.1111/cts.13278)